Growth inhibitory role of the p53 activator SCH 529074 in non-small cell lung cancer cells expressing mutant p53

MILJANA NENKOV[1], YUNXIA MA[1], DANIELA HAASE[1], ZHONGWEI ZHOU[2,3], YONG LI[1], IVER PETERSEN[4], GUANGHUA LU[5] and YUAN CHEN[1]

[1]Section Pathology of The Institute of Forensic Medicine, University Hospital Jena, Friedrich Schiller University, D-07747 Jena; [2]Leibniz Institute on Ageing-Fritz Lipmann Institute (FLI), D-07745 Jena, Germany; [3]School of Medicine (Shenzhen), Sun Yat-Sen University, Guangzhou, Guangdong 510006, P.R. China; [4]Institute of Pathology, SRH Wald-Klinikum, D-07548 Gera, Germany; [5]School of Ethnic Medicine, Chengdu University of Traditional Chinese Medicine, Chengdu, Sichuan 611137, P.R. China

Received January 24, 2019; Accepted December 13, 2019

DOI: 10.3892/or.2020.7546

Abstract. Mutations of p53 occur in approximately 50% of advanced non-small cell lung cancer (NSCLC) cases, leading to loss of tumor suppressive function and/or gain of p53 oncogenic activity. Reactivation of mutant p53 and consequently induction of apoptosis in cancer cells is the goal of p53-targeted therapy. Recently, several p53 mutant reactivating compounds were discovered including SCH 529074. However, the role of SCH 529074 in NSCLC has not been fully explored. In the present study, the effects of this compound on cell survival, cell cycle progression, induction of apoptosis and modulation of cell signaling in p53 mutant NSCLC cells (H1975, H322 and H157) and p53 wild-type NSCLC cells (A549), was investigated. Cell-based functional assays, real-time RT-qPCR and western blot assays were used. HCT116 [p53 wild-type (WT)] and HCT116 $p53^{-/-}$ (p53 null) were used as control cells. The results demonstrated that SCH 529074 treatment caused significant reduction in cell viability and colony formation activity in p53 mutant, p53 WT and p53-deficient cells. The treatment of NSCLC cells with SCH 529074 resulted in a dose-dependent induction of apoptosis and G0/G1 cell cycle arrest, which was associated with the activation of caspases (3 and 7), p53-independent upregulation of p21 and PUMA as well as increased LC3II, a biomarker of autophagy. The combination treatment with the autophagy inhibitor chloroquine (CQ) and SCH 529074 led to decreased cell viability, colony formation and increased induction of apoptosis. The data indicated that SCH 529074 may exert its growth inhibitory function in a p53-independent manner in NSCLC cells.

Correspondence to: Dr Yuan Chen, Section Pathology of The Institute of Forensic Medicine, University Hospital Jena, Friedrich Schiller University, Am Klinikum 1, D-07747 Jena, Germany
E-mail: yuan.chen@med.uni-jena.de

Key words: non-small cell lung cancer, p53 mutations, SCH 529074, apoptosis, autophagy

Introduction

Lung cancer is the most common cause of cancer-related deaths, and every year 1.6 million cases result to fatalities due to this disease (1). Lung cancer is histologically classified into non-small cell lung cancer (NSCLC) which is observed in up to 85% of all lung cancer cases diagnosed, and small-cell lung cancer (SCLC) which accounts for 15% of the remaining cases (2). Only 15% of lung cancer cases are diagnosed at an early stage for which a complete surgical resection is a curative treatment (3). Lung tumors that are present in the advanced stage of the disease are additionally treated with chemotherapy and radiotherapy that may aid the reduction of the tumor size and the symptoms of the disease. However, this type of therapy may cause serious side-effects. During the past 10 years, targeted therapy has been used with EGFR tyrosine kinase inhibitors (TKIs) for patients with activating EGFR mutations, and with ALK inhibitors for patients with abnormal fusion of the anaplastic lymphoma kinase (ALK). These compounds have demonstrated increased therapeutic efficacy and reduced side effects compared with those of chemotherapy in NSCLC patients. However, the patients treated with TKIs develop drug resistance usually within 6-12 months (4). Therefore, the development of more effective therapeutic agents is urgently required for the management of NSCLC.

The tumor suppressor protein p53 is a transcription factor that downregulates the expression levels of the genes associated with tumor development and progression. TP53 exerts functions in the regulation of the cell cycle, apoptosis, senescence and cell metabolism, and is activated in response to cellular stress stimuli, such as DNA damage, oncogenic signaling and mitotic stress (5). Mutations in the *p53* gene occur frequently in various types of human cancer including lung cancer (6). The most common type of *p53* mutations are missense mutations which localize to the DNA binding domain of the gene sequence (exon 5-8). Mutations in the *p53* gene lead to loss of tumor suppressive function and/or gain of oncogenic function that contribute to tumor cell growth, survival, metastasis and drug resistance (7). In lung cancer patients, it has been

demonstrated that p53 mutations are associated with poor prognosis (8). Mutant p53 protein accumulates in tumors and the restoration of its activity can cause cell growth inhibition (9).

In the present study, the tumor inhibitory effects of SCH 529074, one of the p53 restoring compounds initially discovered using drug screening based on p53 DNA binding assays (10), was investigated. SCH 529074 was capable of restoring DNA binding activity of mutant p53 and inhibiting Mdm2 (murine double minute 2) ubiquitination of wild-type (WT) p53. Moreover, this compound affected p53 WT cells (10,11). Due to the high prevalence of p53 mutations in NSCLC and the lack of effective treatment for this cancer type, the reactivation of mutant p53 may provide a novel therapeutic approach. The aim of the present study was to assess the role of SCH 529074 in NSCLC cells with different p53 mutations and explore the molecular alterations caused by this type of drug treatment.

Materials and methods

Cell lines and cell culture. The NSCLC cell lines (A549, H157, H322 and H1975) were obtained from the American Type Culture Collection (ATCC) whereas colon cancer cell lines (HCT116 and HCT116 $p53^{-/-}$) were a gift from Professor Berit Jungnickel (Institute of Cell Biology, Faculty of Biology and Pharmacy, Friedrich Schiller University, Jena). The NSCLC cell lines were grown in RPMI-1640 medium supplemented with 10% (v/v) fetal bovine serum (Biochrom). The colon cancer cell lines were grown in Leibovitz's L-15 medium supplemented with 10% (v/v) fetal bovine serum as previously described (12). The cells were maintained in a humidified atmosphere with 5% CO_2 at 37˚C.

Mutation analysis. Genomic DNA was extracted from the cell lines using the Maxwell® 16 FFPE Tissue LEV DNA Purification Kit (Promega Corp.) according to the manufacturer's instructions. The Maxwell® 16 LEV Instrument was used for genomic analysis. The concentration and purity (260/280 nm ratio) of the genomic DNA were measured using Nano Drop (VWR).

The exons 5-9 of the *p53* gene were amplified using gene specific primers (Table SI) and Hotstart Taq polymerase (VWR). The PCR products were purified using DNA Clean & Concentrator™-5 kit (Zymo Research) according to the manufacturer's recommendations. Purified PCR products (70-90 ng) were subsequently sequenced bidirectionally based on capillary electrophoresis (LGC Genomics GmbH). The sequencing profiles were analyzed with the Finch TV 1.4.0 software program (Geospiza; PerkinElmer).

Drugs. SCH 529074 [N3-[2-[[4-[Bis(4-chlorophenyl) methyl]-1-piperazinyl]methyl]-4-quinazolinyl]-N1, N1-dimethyl-1,3-propanediamine] was purchased from Tocris Bioscience. Doxorubicin was purchased from LC Laboratories. Chloroquine (CQ) was purchased from Sigma Aldrich; Merck KGaA.

Functionality assay of p53. The functionality of p53 in the investigated cell lines was determined by doxorubicin treatment. The cells were seeded in 6-well plates and treated with increasing concentrations of doxorubicin (0.5, 1 and 2 μM) for 24 h. The cells were harvested and the cell lysate was prepared for western blot analysis.

Trypan blue exclusion test for cell viability. The cells ($1x10^5$/well) were seeded into 12-well plates. The following day, the cells were treated with different concentrations of SCH 529074 (2 and 4 μM) or DMSO (0.1%) for 24 h and stained with 0.4% trypan blue solution at room temperature for 5 min (Invitrogen; Thermo Fisher Scientific, Inc.). The number of viable cells was determined by an automated cell counter Countess (Invitrogen; Thermo Fisher Scientific, Inc.) according to the manufacturer's instructions.

Colony formation assay. The cells were seeded into 6-well plates at a density of 2,000 cells/well. Following 24 h of culture, the cells were treated with 1 μM of SCH 529074 or DMSO and were incubated for 8-12 days until colonies were formed. The colonies (at least 50 cells per colony were fixed with 100% of methanol and stained with crystal violet (0.5%) at room temperature for 30 min. The stained colonies were visualized by light microscopy (Zeiss AG).

Cell cycle and apoptosis analyses by flow cytometry. To determine the effect of SCH 529074 on the cell cycle, the cells ($4x10^5$/well) were seeded into 6-well plates and treated with SCH 529074 (2 and 4 μM) or DMSO (0.1%). The following day, the cells ($1\text{-}2x10^6$) were fixed in 70% ethanol following trypsinization and stored at -20˚C overnight. The cells were then stained with propidium iodide (PI) solution (1 μg/μl; BD Biosciences) and analyzed by flow cytometry as previously described (13).

Caspase-3/7 activity assay. The caspase-3/7 activity assay was applied to determine the extent of apoptosis. The cells ($2x10^4$/well) were seeded into 96-well plates and treated with SCH 529074 (4 μM) or DMSO (0.1%) for 24 h. A total of 100 μl of caspase-3/7 reagents was added to each well and the samples were shaken for 30 sec. The reagents were obtained from the Caspase-Glo® 3/7 Assay kit (Promega Corp.). Following incubation of the cells at room temperature (RT) for 2 h, luminescence was recorded with the LUMIstar Galaxy (BMG Labtech).

Quantitative real-time RT-PCR (RT-qPCR). Total RNA was isolated from the cells using peqGOLD TriFastTM (Peqlab) following the manufacturer's instructions. A total of 500 ng of RNA was used for first-strand cDNA synthesis by the QuantiTect Reverse Transcription Kit (Qiagen, Inc.). With regard to the expression analysis, qPCR was conducted on the Rotor-Gene Q (Qiagen, Inc.) using FastStart Universal SYBR Green Master (Roche Diagnostics) with the following conditions: 95˚C 5 sec, 40 cycles of 95˚C 5 sec and 60˚C 1 min. The housekeeping gene *glyceraldehyde-3-phosphate dehydrogenase* (*GAPDH*) was used for normalization of the gene expression data. The $2^{-\Delta\Delta Cq}$ method was used for quantification (14). The data were derived from three independent experiments. The sequences of the primers are listed in Table SI.

Western blotting. The cells ($4x10^5$/well) were seeded into 6-well plates and incubated overnight. The following day, the cells were treated with SCH 529074 (2, 4 and 6 μM) or DMSO for 24 h, harvested and lysed using RIPA buffer (Sigma Aldrich; Merck KGaA). The concentration of protein was determined by using a BCA protein assay kit. Total protein (30-50 μg) was separated by 8% of sodium dodecyl sulfate polyacrylamide gel electrophoresis (SDS-PAGE) and transferred to a AmershamTM ProtranTM 0.2 μM nitrocellulose membrane using a TransBlot® Transfer System (Bio-Rad Laboratories, Inc.). The membranes were blocked for 1 h with 5% BSA or 5% non-fat dry milk in TBST and probed overnight with primary antibodies for p53, p-p53, p21, PUMA, LC3 A/B and actin (Table SII) at 4˚C. The membranes were washed with TBST and incubated with secondary antibodies for 1 h at RT. Finally, the immunoreactivity was visualized using an enhanced chemiluminescence detection system (GE Healthcare). The signals were quantified using Image Studio Lite Version 5.2.5 (LI-COR Biosciences).

Statistical analysis. Statistical analysis was performed using the software package SPSS 19.0 (IBM Corp). The differences between the single drug-treated and control samples were assessed using the Student's t-test. For combination drug therapy, two-way ANOVA (with Tukey's multiple comparisons test) was performed using GraphPad Prism 7.04 (GraphPad Software, Inc.). P<0.05 was considered to indicate statistically significant differences.

Results

TP53 mutation status and p53 protein expression in NSCLC cell lines. TP53 mutation was confirmed in three (H1975, H322 and H157) cell lines. Direct sequencing of the *p53* gene confirmed the presence of the 'CGT>CAT' (R273H), 'CGG>CTG' (R248L) and 'CAG>TAG' (298stop) mutations in H1975, H322 and H157 cells, respectively (Fig. S1A). The WT TP53 status was observed in both A549 and HCT116 cells (Fig. S1B). High levels of the mutant p53 protein were detected in H1975, H322, A549 and HCT116 cells. As anticipated the p53 protein was present in neither HCT116 $p53^{-/-}$ nor H157 cells due to deletion or non-sense mutation of p53 in the two cell lines. The expression of *p53* mRNA in these two cell lines (data not shown) was also not detected. To assess the functionality of p53 in these cell lines, the levels of the phosphorylated p53 protein (p-p53) and the expression levels of the p53 target gene *p21* were analyzed following doxorubicin treatment. The induction of the p-p53 levels and the expression levels of p21 were present in the WT cell lines (A549 and HCT116), and only weak signals were detected in the mutant cell lines (H1975 and H322). The p53-deficient cell line (HCT116 $p53^{-/-}$) or the cell line with the 298stop (H157) codon did not express p53 or p21 proteins (Fig. S2).

SCH 529074 inhibits cancer cell viability and colony formation. To evaluate the effects of the drugs on tumor cell growth, the cell survival assay was performed. Reduced cell viability was observed in all tested NSCLC cell lines treated with 2 and 4 μM of SCH 529074 (Fig. 1A). Upon treatment with the higher concentration (4 μM) of this compound, the viability of the cells was significantly decreased to 20-25% in p53 mutant cells (H157, H1975 and H322, P<0.001) and to 68% in the p53 WT cell line A549 (P=0.032) compared with that observed in the control cells.

Subsequently, the toxicity of SCH 529074 to NSCLCs was investigated by colony formation assay, which is commonly used for determining the efficacy of cytotoxic drugs and for testing the ability of the cells to undergo unlimited divisions (15). The data indicated that SCH 529074 treatment significantly reduced the ability of cancer cells to form colonies (Fig. 1B). The colony formation activity of SCH 529074-treated cells was reduced to 19 and 23% (P<0.001) in H322 and H1975 cells, respectively, compared with that of the control cells. In H157 and A549 cells, this parameter was reduced to 41% (P<0.001) and 58% (P=0.0003), respectively, compared with that of the control cells. Similarly, colony formation activity was reduced to 30% (P<0.001) in HCT116 cells and to 70% (P=0.0034) in HCT116 $p53^{-/-}$ cells compared with that of the control cells. These data indicated that p53 mutant cells were more sensitive to SCH 529074 treatment compared with the p53 WT NSCLC cells. Notably, upon SCH529074 treatment, the p53 null mutant cell line (H157) was sensitive to a short-term effect as demonstrated by the cell viability assay (Fig. 1A) and more resistant to long-term effects as demonstrated by the colony formation assay (Fig. 1B).

SCH 529074 induces G0/G1 cell cycle arrest. Due to the important role of p53 in cell cycle regulation and the observed growth inhibitory effects of SCH 529074, its effects were further investigated on cell cycle progression. Fig. 2A revealed the cell cycle profiles of H157 cells following different treatment concentrations. NSCLC cells (H157, A549, HCT116 and HCT116 $p53^{-/-}$) were arrested at the G0/G1 phase (59%, P<0.001; 72%, P<0.001; 66%, P<0.001; and 57%, P<0.001) compared with the control cells following low concentration (2 μM) of drug treatment (Fig. 2B). This G0/G1 phase arrest was not observed in the two p53 mutant NSCLC cell lines (H1975 and H322). Treatment of the cells with high SCH 529074 concentration (4 μM) resulted in a significantly increased G0/G1 phase and a decreased S phase. These effects were observed in all the different cell lines assessed regardless of the p53 status. In addition, an increased sub-G1 subpopulation was further observed in all NSCLC cell lines following treatment with 4 μM of SCH 529074 (Fig. 2B) indicating the induction of apoptosis in these cells.

SCH 529074 induced apoptosis in cancer cells. To confirm the effects of SCH 529074 on cancer cell apoptosis, flow cytometric analysis was carried out following Annexin V/PI double staining. Upon SCH 529074 treatment (4 μM), the early apoptotic fraction was increased to ~10% (P<0.001) in H322 cells compared with those of the control cells (Fig. 3A and B). In H1975 cells treated with SCH 529074 (2 μM), the early and late apoptotic rates were significantly increased compared with that of the control cells (P<0.05 and P<0.01), and following treatment with high concentration of the compound (4 μM), both early and late apoptotic rates were significantly enhanced (P<0.01 and P<0.001). In H157 cells, 2 μM of SCH 529074 treatment induced early and late apoptosis (P<0.001 and P<0.05), and 4 μM of this compound also induced early and late apoptosis (P<0.05 and P<0.01). Similarly, in A549 cells,

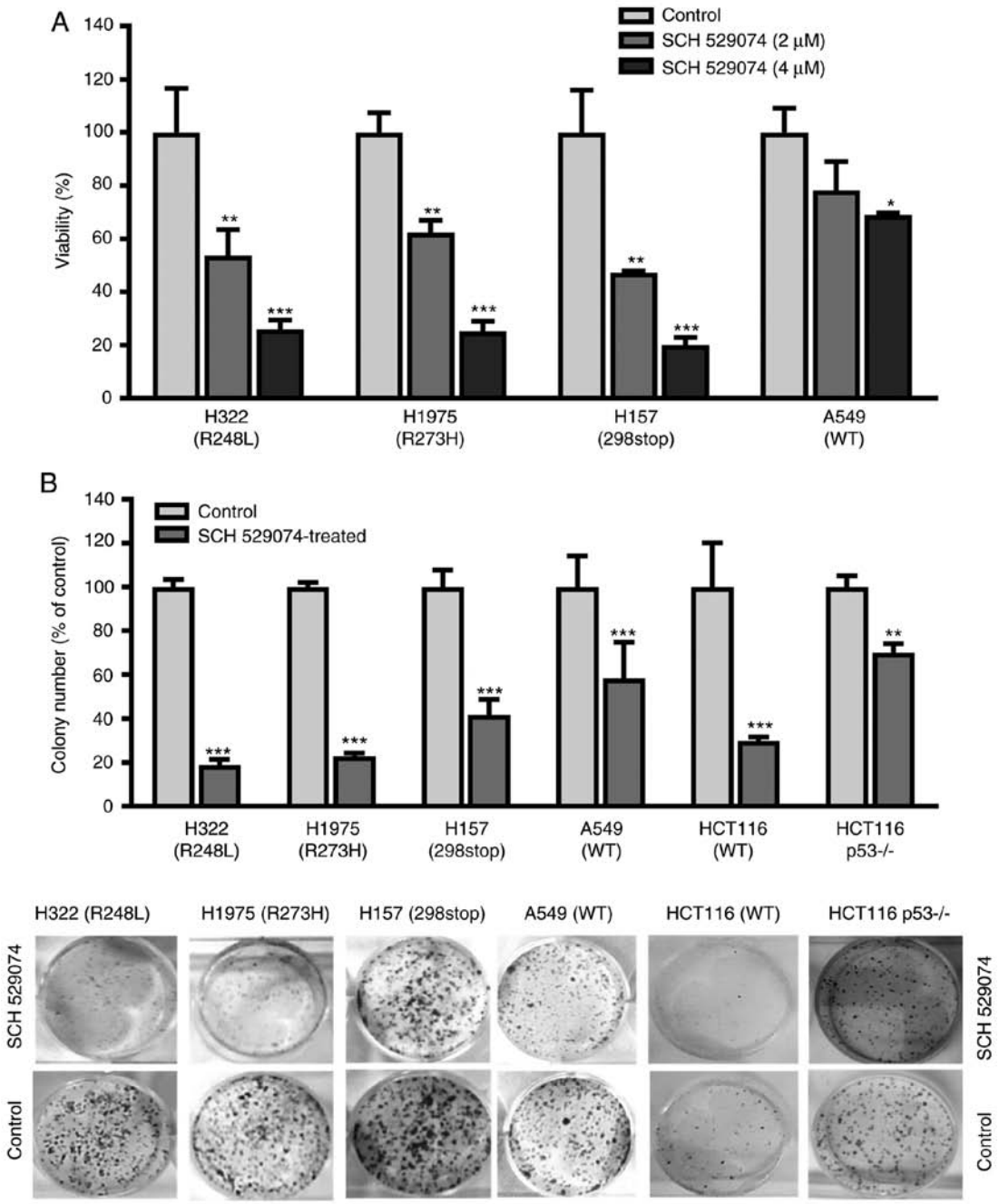

Figure 1. Inhibitory effects of SCH 529074 on cancer cell viability and colony formation. (A) Reduction of cancer cell survival (%) upon drug treatment with different concentrations. (B) Quantitative analysis of colony formation (upper images) and representative images (lower images). The data are presented as the mean of three independent experiments ± standard deviation (SD). *P<0.05, **P<0.01 and ***P<0.001 when analyzed with the Student's t-test.

2 and 4 μM of SCH 529074 significantly increased early and late apoptosis (P<0.01 and P<0.05 for 2 μM; P<0.001 and P<0.01 for 4 μM). These data revealed that SCH 529074 could induce apoptosis in all assessed NSCLC cell lines irrespective of their p53 mutational status. In line with that, in colon cancer cells, a significant induction of early and late apoptosis was observed in HCT116 cells at a concentration of 4 μM (P<0.01 and P<0.05), and in HCT116 p53$^{-/-}$ cells, treatment with 4 μM of SCH 529074 significantly induced early apoptosis (P<0.05).

To examine whether the induction of apoptosis was caspase-dependent, a caspase Glo® 3/7 activity assay was used. All NSCLC cell lines demonstrated a significantly higher caspase-3/7 activity following SCH 529074 treatment compared with that of the control cells (P<0.01 and P<0.001; Fig. 3C).

SCH 529074 alters the expression of pro-apoptotic and cell cycle regulatory genes. TP53 has been revealed to induce apoptosis and regulate the cell cycle according to external stimuli, which further cause activation of the p53 responsive genes (16). As a p53 activator, SCH 529074 may induce transcription of the p53 target genes. To examine this, the expression of the p53 downstream apoptosis-associated genes *PUMA*, *NOXA* and *BAX* as well as of the cell cycle-associated genes *p21* and *CCNG2,* were analyzed. As revealed in Fig. 4A, *PUMA* was significantly increased in all the cancer cell lines assessed

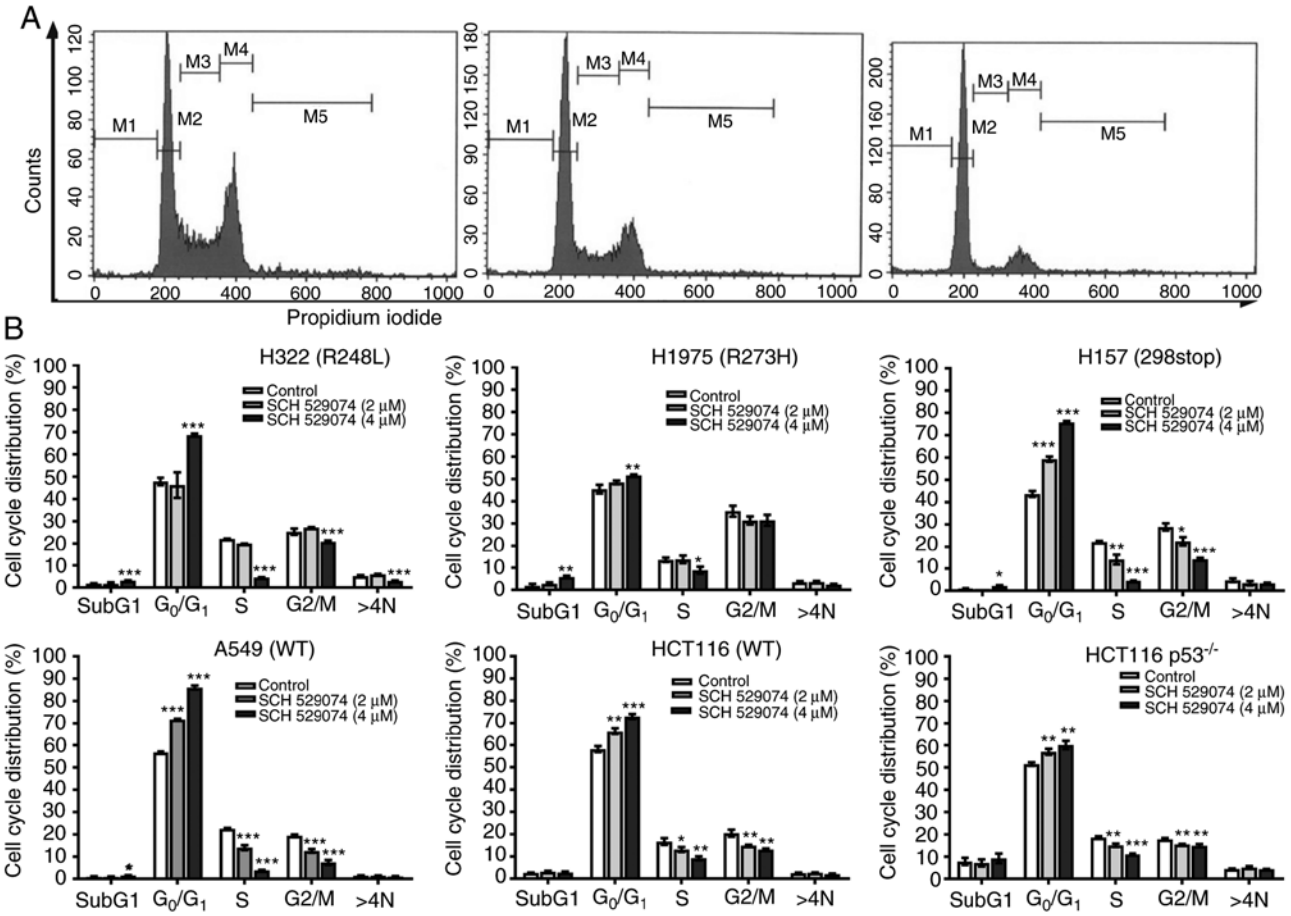

Figure 2. Effects of SCH 529074 on the cell cycle were determined by flow cytometry. (A) Representative DNA histograms on the cell cycle profile of the H157 cell line. (B) Quantitative analysis of distribution of cells in different cell cycle stages. The data are presented as the mean of three independent experiments ± SD. *P<0.05, **P<0.01 and ***P<0.001. The data were analyzed with the Student's t-test.

irrespective of the p53 mutation status. The expression levels of *NOXA* were only upregulated in H1975 cells (R273H). *BAX* expression was not significantly altered following drug treatment (data not shown). The mRNA levels of *p21* and *CCNG2* were increased in all NSCLC cell lines but not in colon cancer cell lines (Fig. 4B). To confirm these results, the protein levels of PUMA and p21 were further analyzed by western blotting. Consistent with the mRNA data, the protein levels of PUMA and p21 were revealed to be increased upon 4 or 6 μM of SCH 529074 treatment in the cancer cell lines regardless of their p53 status (Figs. 4C and S3).

SCH 529074 treatment increases the levels of LC3II. Since p53 can regulate autophagy (17), further experiments assessed the ability of SCH 529074 to affect autophagy. During autophagy, the cytoplasmic form of LC3-I is converted to the autophagosome-associated form of LC3II, which is considered a marker for autophagy (18). As revealed in Fig. 5, treatment with SCH 529074 led to increased LC3-II levels in all tumor cell lines assessed regardless of their p53 mutation status.

Combined treatment with CQ and SCH 529074 increases LC3-II levels, reduces cell survival and enhances induction of apoptosis. A combination treatment of SCH 529074 and the autophagy inhibitor CQ was performed. The cells were treated with a low concentration of SCH 529074 (1 μM) and CQ (15 μM) for 72 h in order to reduce the toxicity caused by the drugs. As revealed in Fig. 6A, the levels of LC3-II were increased in cells treated with SCH 529074 and CQ compared with cells treated with SCH 529074 alone. However, LC3-II levels were similar between the combined treatment and the CQ single treatment. Moreover, combination treatment significantly reduced the ability of NSCLC cells (H1975, H157 and A549) to form colonies compared with that noted by single drug treatment (Fig. 6B). Furthermore, flow cytometric analysis was performed in order to investigate if the combination treatment could synergistically increase the apoptotic rates. SCH 529074 (1 μM) and CQ treatment produced a significantly increased apoptotic rate in H1975 cells (for both P<0.05), whereas the combination treatment resulted in a significantly higher apoptotic rate compared with that observed following single drug treatment of the cells (P<0.01, Fig. 6C).

Discussion

SCH 529074 is a small molecular weight compound that can bind to the p53-DNA binding domain, restore growth-suppressive activity of mutant p53 and interrupt Mdm2-mediated ubiquitination of WT mutant p53 (10). In the present study, the role of SCH 529074 was investigated in NSCLC cells with different p53 mutational status and two colorectal cancer cell lines HCT116 and HCT116 p53$^{-/-}$ were included as controls,

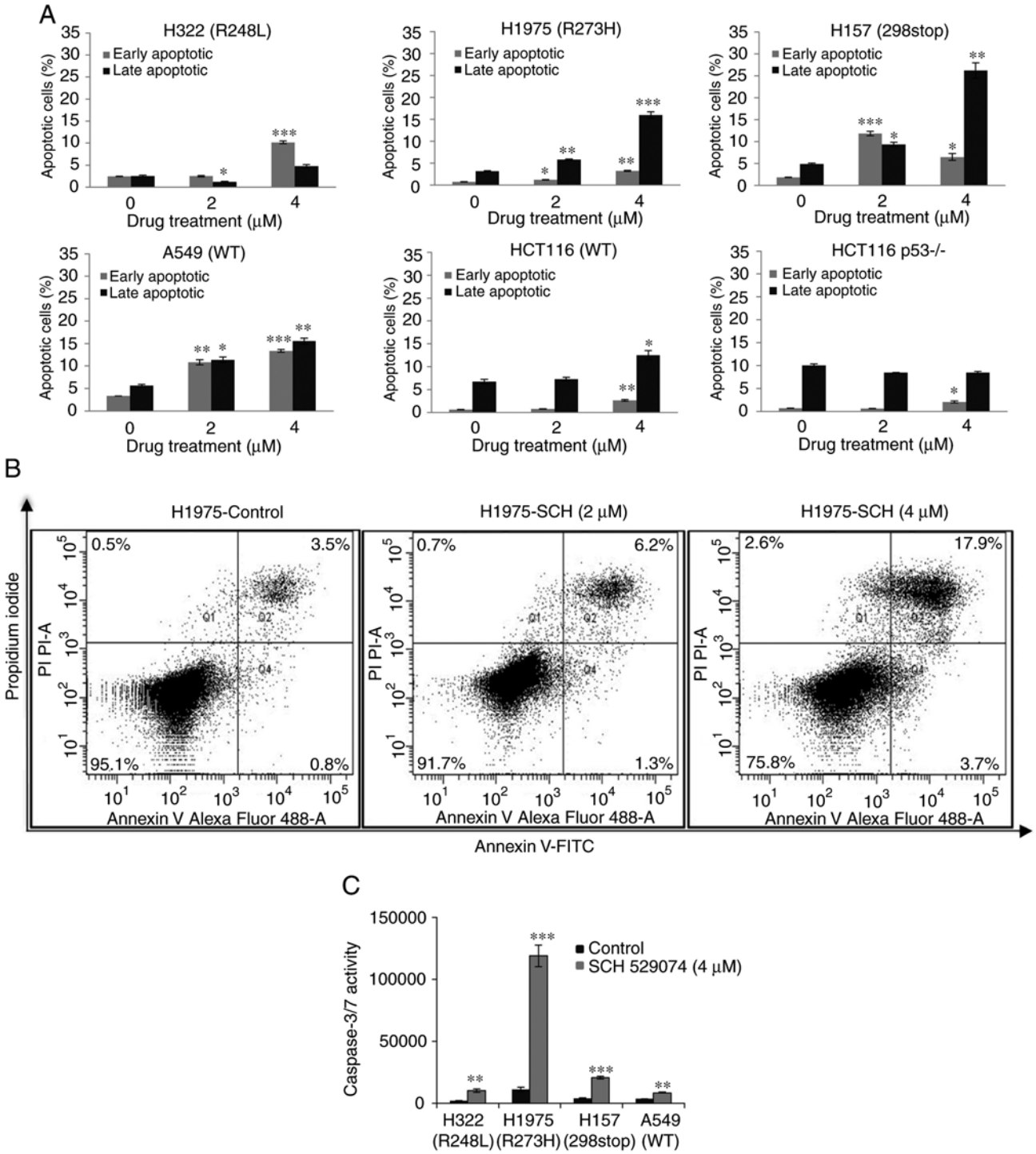

Figure 3. Impact of SCH 529074 treatment on apoptosis. (A) Quantitative analysis of apoptotic cells with regard to the population of cells, the percentage of early apoptotic cells (Annexin V^+ PI^-, Q4) and the percentage of late apoptotic cells (Annexin V^+ PI^+, Q2). (B) Representative dot plots combining Annexin V-FITC and PI fluorescence in H1975 cells treated with SCH 529074. The data indicate the viable cell population in the bottom left quadrant Q3 (Annexin V^- PI^-), the early apoptotic cell population in the quadrant Q4 (Annexin V^+, PI^-) and the population of late apoptotic cells in the Q2 quadrant (Annexin V^+ PI^+). (C) Analysis of the activity of caspase-3/7 using a Caspase-Glo® 3/7 Assay Kit in H1975, H322, H157 and A549 cells treated with SCH 529074. The intensity of luminescence which reflected the caspase-3/7 activity is presented. The experiment was repeated in triplicate. The data are presented as the mean of three independent experiments ± SD. $^*P<0.05$, $^{**}P<0.01$ and $^{***}P<0.001$ when analyzed with the Student's t-test. PI, propidium iodide.

since these paired cell lines have been widely applied to analyze the function of p53 (19,20).

Initially, the mutation status and protein expression levels of p53 were assessed in 4 lung cancer and 2 colon cancer cell lines. A high protein level of p53 was detected in H1975 (R273H) and H322 (R248L) cells. Mutant p53 fails to induce transcription of its negative regulator Mdm2, leading to loss of ubiquitination and reduced degradation by Mdm2 (21). This results to an accumulation of p53 in these cells (21). In line with these findings, it was revealed that the two p53 WT cell lines (A549 and HCT116) exhibited low levels of p53, which could be attributed to its degradation by Mdm2. Notably,

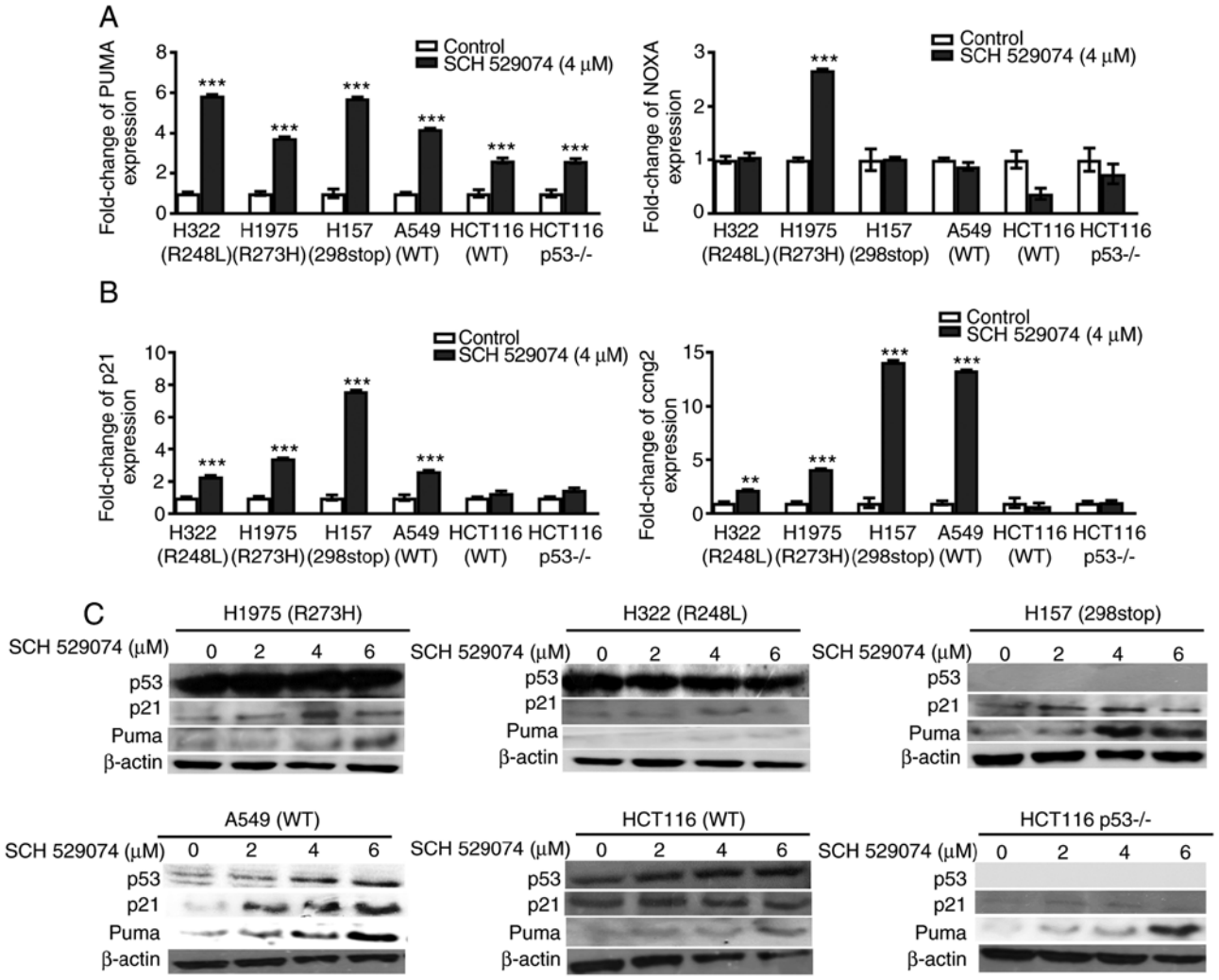

Figure 4. Induction of pro-apoptotic genes and cell cycle regulatory genes by SCH 529074. (A and B) The mRNA expression levels of the pro-apoptotic genes (*PUMA* and *NOXA*) and of the cell cycle regulators (*p21* and *CCNG2*) were analyzed by real-time RT-qPCR. The data are presented as the mean of three independent experiments ± SD. **P<0.01, ***P<0.001 following analysis with the Student's t-test. (C) The protein expression levels of p53, p21 and PUMA following SCH 529074 treatment. β-actin was used as a loading control.

p53 expression was not detectable in H157 cells containing a heterogeneous mutant (298stop) form of p53. This phenomenon may be caused by epigenetic modification of p53 and/or p53 regulatory genes. Regardless of the p53 mutation status, suppressed cell survival was observed in all these cell lines including HCT116 $p53^{-/-}$, which was associated with a reduced colony formation activity following drug treatment, suggesting that SCH 529074 inhibited cell survival in a p53-independent manner.

p53 is involved in regulating the cell cycle and in the induction of apoptosis (5). SCH 529074 treatment resulted in G0/G1 cell cycle arrest irrespective of the p53 status of the cells. The cell cycle is strictly regulated by cell cycle regulators, such as cyclins, CDKs (cyclin-dependent kinase), and CDKIs (cyclin-dependent kinase inhibitors) (22). Following SCH 529074 treatment, one of the cyclin-dependent kinase inhibitors p21 was upregulated at both the mRNA and protein level in all assessed NSCLC cell lines. The *p21* gene was initially reported to induce cell cycle arrest by mediating p53-dependent G1 growth arrest (23). It has also been revealed that p21 is an effector of multiple pathways required for promoting p53-independent anti-proliferative activities (23). The p53-independent induction of p21 could be achieved through downregulation of c-Myc (24). In contrast to other cyclins, which play roles in cell cycle progression, G cyclins negatively regulate cell proliferation (25). The data indicated that NSCLC cells expressed significantly higher levels of *CCNG2* mRNA following drug treatment and that its expression was notably high in H157 (298stop) and A549 (p53 WT) cells. Decreased expression of CCNG2 was detected in various tumors including lung cancer, and it was correlated with lymph node metastasis and poor overall survival (26). Notably, SCH 529074 treatment did not alter the expression levels of p21 and CCNG2 in colon cancer cells, indicating a tissue specific effect/mechanism. The data revealed that SCH 529074 treatment induced a p53-independent cell cycle arrest and an altered expression of cell cycle-associated genes in lung cancer cells.

In addition to the effects of SCH 529074 on cell cycle arrest, induction of apoptosis was observed in all NSCLC cells via a p53-independent manner. A dose-response effect was observed with regard to SCH 529074 treatment and the

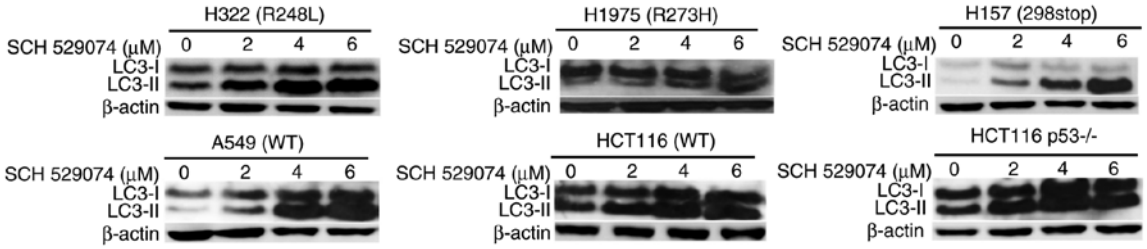

Figure 5. Induction of LC3-II expression by SCH 529074 treatment of lung cancer cells. The protein levels of LC3I and LC3II were assessed by western blot analysis. β-actin was used as a loading control.

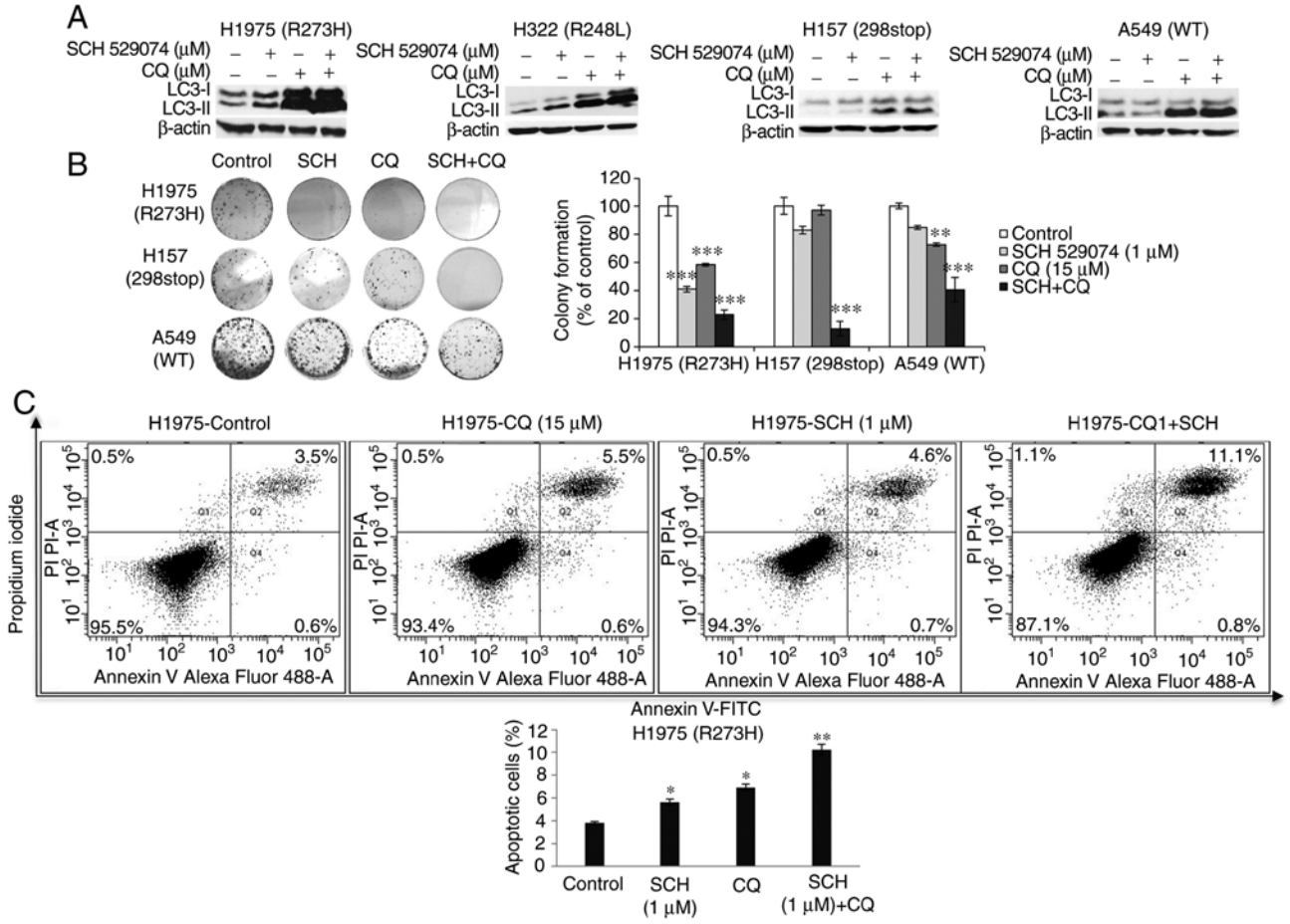

Figure 6. Effects of SCH 529074 and CQ treatment on colony formation, induction of apoptosis and LC3-II protein levels in NSCLC cell lines. (A) The protein expression levels of LC3-I and LC3-II were analyzed by western blotting. β-actin was used as a loading control. (B) The effects of CQ and SCH 529074 on colony formation. Representative images of crystal violet-stained colonies of NSCLC cells. Quantified colonies are presented as a percentage to the control cells. Mean ± SD is presented. **P<0.01 and ***P<0.001 following analysis with the Student's t-test. (C) The effects of SCH 529074 and CQ on the induction of apoptosis in the H1975 cell line. The percentage of apoptotic cells was assessed using Annexin V/PI staining and analyzed by flow cytometry. Representative dot plots of Annexin V/PI staining are presented (upper images). The quantification of Annexin V/PI staining including the early and late apoptotic populations is presented (lower image). The data are presented as the mean of three independent experiments ± SD. *P<0.05, **P<0.01 following analysis with the Student's t-test. CQ, chloroquine; PI, propidium iodide.

induction of apoptosis, which was accompanied by increased caspase-3/7 activity. Although p53 is the one of the key players in the apoptotic pathway, other supplementary pathways independent of p53 exist (27). However, the cell lines (H157 and A549) that exhibited the highest apoptotic rate did not exhibit the highest caspase-3/7 activity, suggesting that SCH 529074-induced apoptosis may be mediated by both caspase-dependent and -independent pathways in these cells. The induction of apoptosis is activated when the expression of the pro-apoptotic proteins (PUMA, NOXA, BAX, BIM, BAD and BID) overcomes the expression of the anti-apoptotic proteins (BCL-2, BCL-xl, MCl-1 and BCL-W) (28). PUMA is a BH3-only protein and a critical mediator of the p53-dependent and -independent apoptotic pathways (29). For example, Wu *et al* revealed that p53 independent induction of PUMA mediated intestinal apoptosis in response to ischemia-reperfusion (30). Upon treatment of SCH 529074, PUMA mRNA and protein levels were upregulated in all cancer cell lines

regardless of their p53 status, indicating that SCH 529074 induced a p53-independent expression of PUMA. In HCT116 $p53^{-/-}$ cells treated with 2 μM of SCH 529074, no apoptosis was present, but when these cells were treated with 4 μM of SCH 529074, a significantly higher early apoptotic rate was detected, in line with the increased expression level of PUMA in this cell line. It is reported that PUMA alone was not sufficient to induce apoptosis. This may be due to a change in the subcellular localization of the PUMA protein. Ambroise *et al* observed that neither PUMA upregulation in normal activated human B lymphocytes, nor high levels of PUMA in Burkitt's lymphoma cells were associated with cell death (31). This was due to the subcellular localization of PUMA occurring in the cytosol and not in the mitochondria (31). Increased PUMA levels potently induce apoptosis by antagonizing the expression levels of the anti-apoptotic Bcl-2 family members and/or by directly activating the pro-apoptotic protein members, leading to mitochondrial dysfunction and initiation of the caspase activation cascade (32). In contrast to the enhanced expression of PUMA observed in all assessed cell lines, no significant alteration of BAX expression was observed. Moreover, NOXA was induced only in p53 mutant H1975 cells, which may be associated with the genetic feature of the cell line including mutation status of p53, p53-regulatory genes and genes interacting with p53 (33). The expression levels of p53 were not markedly altered in mutant cell lines, although they did change in the WT cell lines A549 and HCT116, possibly due to the ability of the compound to interrupt Mdm2-mediated ubiquitination of WT p53 (10). Collectively, the data indicated that SCH 529074 may induce both p53-dependent and -independent apoptosis. Similarly, a pre-clinical study also reported that NJ-26854165 (Serdemetan), a p53 activating tryptamine derivative, had growth inhibitory activities in both wild-type and mutant p53 tumors, indicating that the mechanism involves both p53-dependent and -independent functions (34).

Several studies have reported that genotoxic stimuli could trigger autophagy in cancer cells. Cordani *et al* reported that mutant p53 interacted with the induction of autophagy during cancer progression (35). The present study revealed that SCH 529074 treatment caused increased LC3-II levels regardless of the p53 mutational status, indicating its potential involvement in autophagy. However, the LC3-II levels in the cells treated by SCH 529074 and the autophagy inhibitor CQ were similar to those observed in the cells treated with CQ alone, which was possibly due to the fact that the autophagy inhibitor may have caused the inhibition of the autophagosome-lysosome fusion, leading to accumulation of LC3-II (36,37). Nevertheless, combination treatment with low concentration of SCH 529074 and the autophagy inhibitor CQ led to reduced tumor cell survival rates compared with those observed following single drug treatment, indicating the efficacy of this combination therapy in NSCLC cells. It has been previously revealed that the application of combination therapy can maximize sensitivity and minimize the toxicity observed in the treatment of cancer cells (38). The precise role of SCH 529074 in autophagy requires further investigation by the analysis of additional autophagic markers. Furthermore, the effects of SCH 529074 should also be assessed in normal bronchial epithelial cells and in *in vivo* animal models in future studies.

In summary, the data from the present study indicated that SCH 529074 exerts growth inhibitory effects on NSCLC cells by inducing cell cycle arrest, apoptosis and possibly autophagy. These results were in agreement with those reported by Demma *et al* (10). However, it was demonstrated that this compound further exhibited effects on p53-deficient cells, indicating a p53-independent mechanism of action. Additionally, the ability of SCH 529074 to induce autophagy is a novel finding. SCH 529074 bears therapeutic potential and may be used in combination with a low concentration of other drugs for the treatment of patients with lung cancer.

Acknowledgements

We thank Professor Berit Jungnickel for kindly providing us with the colon cancer cell lines HCT116 and HCT116 $p53^{-/-}$. We thank Claudia Seliger for technical support.

Funding

The present study was supported by University Hospital Jena.

Availability of data and materials

The datasets used and/or analyzed during the current study are available from the corresponding author on reasonable request.

Authors' contributions

YC, IP and GL conceived and designed the study. MN, DH, ZZ, YL and YM performed the experiments. YM was responsible for data analysis and preparation of the figures. MN and YC wrote the manuscript. All authors read and approved the manuscript and agree to be accountable for all aspects of the research in ensuring that the accuracy or integrity of any part of the work are appropriately investigated and resolved.

Ethics approval and consent to participate

Not applicable.

Patient consent for publication

Not applicable.

Competing interests

The authors declare that they have no competing interests.

References

1. Hirsch FR, Scagliotti GV, Mulshine JL, Kwon R, Curran WJ Jr, Wu YL and Paz-Ares L: Lung cancer: Current therapies and new targeted treatments. Lancet 389: 299-311, 2017.
2. Oser MG, Niederst MJ, Sequist LV and Engelman JA: Transformation from non-small-cell lung cancer to small-cell lung cancer: Molecular drivers and cells of origin. Lancet Oncol 16: e165-e172, 2015.
3. Mascaux C, Tomasini P, Greillier L and Barlesi F: Personalised medicine for nonsmall cell lung cancer. Eur Respir Rev 26: 170066, 2017.
4. Lin Y, Wang X and Jin H: EGFR-TKI resistance in NSCLC patients: Mechanisms and strategies. Am J Cancer Res 4: 411-435, 2014.

5. Green DR and Chipuk JE: p53 and metabolism: Inside the TIGAR. Cell 126: 30-32, 2006.
6. Mogi A and Kuwano H: TP53 mutations in nonsmall cell lung cancer. J Biomed Biotechnol 2011: 583929, 2011.
7. Brosh R and Rotter V: When mutants gain new powers: News from the mutant p53 field. Nat Rev Cancer 9: 701-713, 2009.
8. Steels E, Paesmans M, Berghmans T, Branle F, Lemaitre F, Mascaux C, Meert AP, Vallot F, Lafitte JJ and Sculier JP: Role of p53 as a prognostic factor for survival in lung cancer: A systematic review of the literature with a meta-analysis. Eur Respir J 18: 705-719, 2001.
9. Yue X, Zhao Y, Xu Y, Zheng M, Feng Z and Hu W: Mutant p53 in cancer: Accumulation, gain-of-function and therapy. J Mol Bio 429: 1595-1606, 2017.
10. Demma M, Maxwell E, Ramos R, Liang L, Li C, Hesk D, Rossman R, Mallams A, Doll R, Liu M, *et al*: SCH529074, a small molecule activator of mutant p53, which binds p53 DNA binding domain (DBD), restores growth-suppressive function to mutant p53 and interrupts HDM2-mediated ubiquitination of wild type p53. J Bio Chem 285: 10198-10212, 2010.
11. Parrales A and Iwakuma T: Targeting oncogenic mutant p53 for cancer therapy. Front Oncol 5: 288, 2015.
12. Cui T, Chen Y, Yang L, Knösel T, Zöller K, Huber O and Petersen I: DSC3 expression is regulated by p53, and methylation of DSC3 DNA is a prognostic marker in human colorectal cancer. Br J Cancer 15: 1013-1019, 2011.
13. Li Y, Chen Y, Ma Y, Nenkov M, Haase D and Petersen I: Collagen prolyl hydroxylase 3 has a tumor suppressive activity in human lung cancer. Exp Cell Res 363: 121-128, 2018.
14. Livak KJ and Schmittgen TD: Analysis of relative gene expression data using real-time quantitative PCR and the 2(-Delta Delta C(T)) method. Methods 25: 402-408, 2001.
15. Franken NA, Rodermond HM, Stap J, Haveman J and van Bree C: Clonogenic assay of cells in vitro. Nat Protoc 1: 2315-2319, 2006.
16. Weinberg RA: p53 and apoptosis: Master guardian and executioner. The Biology of Cancer, Garland Science, Taylor & Francis Group, New York, NY, pp331-389, 2014.
17. Levine B and Abrams J: p53: The Janus of autophagy? Nat Cell Biol 10: 637-639, 2008.
18. Tanida I, Ueno T and Kominami E: LC3 and autophagy. Methods Mol Biol 445: 77-88, 2008.
19. Zhou X, Hai Q and Lu H: Mutant p53 in cancer therapy-the barrier or the path. J Mol Cell Biol 11: 293-305, 2019.
20. Lee YS, Yoon S, Park MS, Kim JH, Lee JH and Sonog CW: Influence of p53 expression on sensitivity of cancer cells to bleomycin. J Biochem Mol Toxicol 24: 260-269, 2010.
21. Bykov VJ, Issaeva N, Shilov A, Hultcrantz M, Pugacheva E, Chumakov P, Bergman J Wiman KG and Selivanova G: Restoration of the tumor suppressor function to mutant p53 by a low-molecular-weight compound. Nat Med 8: 282-288, 2002.
22. Vermeulen K, Van Bockstaele DR and Berneman ZN: The cell cycle: A review of regulation, deregulation and therapeutic targets in cancer. Cell Prolif 36: 131-149, 2003.
23. Karimian A, Ahmadi Y and Yousefi B: Multiple functions of p21 in cell cycle, apoptosis and transcriptional regulation after DNA damage. DNA Repair (Amst) 42: 63-71, 2016.
24. Jeong JH, Kang SS, Park KK, Chang HW, Magae J and Chang YC: p53-independent induction of G1 arrest and p21WAF1/CIP1 expression by ascofuranone, an isoprenoid antibiotic, through downregulation of c-Myc. Mol Cancer Ther 9: 2102-2113, 2010.
25. Arachchige Don AS, Dallapiazza RF, Bennin DA, Brake T, Cowan CE and Horne MC: Cyclin G2 is a centrosome-associated nucleocytoplasmic shuttling protein that influences microtubule stability and induces a p53-dependent. Exp Cell Res 312: 4181-4204, 2006.
26. Sun GG, Zhang J and Hu WN: CCNG2 expression is down-regulated in colorectal carcinoma and its clinical significance. Tumour Biol 35: 3339-3346, 2014.
27. Strasser A, Harris AW, Jacks T and Cory S: DNA damage can induce apoptosis in proliferating lymphoid cells via p53-independent mechanisms inhibitable by Bcl-2. Cell 79: 329-339, 1994.
28. Montero J and Letai A: Why do BCL-2 inhibitors work and where should we use them in the clinic? Cell Death Differ 25: 56-64, 2018.
29. Yu J and Zhang L: PUMA, a potent killer with or without p53. Oncogene 27 (Suppl 1): S71-S83, 2008.
30. Wu B, Qiu W, Wang P, Yu H, Cheng T, Zambetti GP, Zhang L and Yu J: p53 independent induction of PUMA mediates intestinal apoptosis in response to ischaemia-reperfusion. Gut 56: 645-654, 2007.
31. Ambroise G, Portier A, Roders N, Arnoult D and Vazquez A: Subcellular localization of PUMA regulates its pro-apoptotic activity in Burkitt's lymphoma B cells. Oncotarget 6: 3818-3894, 2015.
32. Zheng X, He K, Zhang L and Yu J: Crizotinib induces PUMA-dependent apoptosis in colon cancer cells. Mol Cancer Ther 12: 777-786, 2013.
33. Hafner A, Bulyk ML, Jambhekar A and Lahav G: The multiple mechanisms that regulate p53 activity and cell fate. Nat Rev Mol Cell Biol 20: 199-210, 2019.
34. Smith MA, Gorlick R, Kolb EA, Lock R, Carol H, Maris JM, Keir ST, Morton CL, Reynolds CP, Kang MH, *et al*: Initial testing of JNJ-26854165 (Serdemetan) by the pediatric preclinical testing program. Pediatr Blood Cancer 59: 329-332, 2012.
35. Cordani M, Butera G, Pacchiana R and Donadelli M: Molecular interplay between mutant p53 proteins and autophagy in cancer cells. Biochim Biophys Acta Rev Cancer 1867: 19-28, 2017.
36. Mizushima N and Yoshimori T: How to interpret LC3 immunoblotting. Autophagy 3: 542-545, 2007.
37. Huang S and Sinicrope FA: Celecoxib-induced apoptosis is enhanced by ABT-737 and by inhibition of autophagy in human colorectal cancer cells. Autophagy 6: 256-269, 2010.
38. Matlock K, Berlow N, Keller C and Pal R: Combination therapy design for maximizing sensitivity and minimizing toxicity. BMC Bioinformatics 18 (Suppl 4): S116, 2017.